Computers Math. Applic. Vol. 19, No. 8/9, pp. 127–145, 1990
Printed in Great Britain

0097-4943/90 $3.00 + 0.00
Pergamon Press plc

MULTIQUADRICS—A SCATTERED DATA APPROXIMATION SCHEME WITH APPLICATIONS TO COMPUTATIONAL FLUID-DYNAMICS—I

SURFACE APPROXIMATIONS AND PARTIAL DERIVATIVE ESTIMATES

E. J. KANSA
Lawrence Livermore National Laboratory, L-200, P.O. Box 808, Livermore, CA 94550, U.S.A.

Abstract—We present a powerful, enhanced multiquadrics (MQ) scheme developed for spatial approximations. MQ is a true scattered data, grid free scheme for representing surfaces and bodies in an arbitrary number of dimensions. It is continuously differentiable and integrable and is capable of representing functions with steep gradients with very high accuracy. Monotonicity and convexity are observed properties as a result of such high accuracy.

Numerical results show that our modified MQ scheme is an excellent method not only for very accurate interpolation, but also for partial derivative estimates. MQ is applied to a higher order arbitrary Lagrangian–Eulerian (ALE) rezoning. In the second paper of this series, MQ is applied to parabolic, hyperbolic and elliptic partial differential equations. The parabolic problem uses an implicit time-marching scheme whereas the hyperbolic problem uses an explicit time-marching scheme. We show that MQ is also exceptionally accurate and efficient. The theory of Madych and Nelson shows that the MQ interpolant belongs to a space of functions which minimizes a semi-norm and gives credence to our results.

1. BACKGROUND

The study of arbitrarily shaped curves, surfaces and bodies having arbitrary data orderings has immediate application to computational fluid-dynamics. The governing equations not only include source terms but gradients, divergences and Laplacians. In addition, many physical processes occur over a wide range of length scales. To obtain quantitatively accurate approximations of the physics, quantitatively accurate estimates of the spatial variations of such variables are required. In two and three dimensions, the range of such quantitatively accurate problems possible on current multiprocessing super computers using standard finite difference or finite element codes is limited. The question is whether there exist alternative techniques or combinations of techniques which can broaden the scope of problems to be solved by permitting steep gradients to be modelled using fewer data points. Toward that goal, our study consists of two parts. The first part will investigate a new numerical technique of curve, surface and body approximations of exceptional accuracy over an arbitrary data arrangement. The second part of this study will use such techniques to improve parabolic, hyperbolic or elliptic partial differential equations. We will demonstrate that the study of function approximations has a definite advantage to computational methods for partial differential equations.

One very important use of computers is the simulation of multidimensional spatial processes. In this paper, we assumed that some finite physical quantity, F, is piecewise continuous in some finite domain. In many applications, F is known only at a finite number of locations, $\{\mathbf{x}_k : k = 1, 2, \ldots, N\}$ where $\mathbf{x}_k = x_k$ for a univariate problem, and $\mathbf{x}_k = (x_k, y_k, \ldots)^T$ for the multivariate problem.

From a finite amount of information regarding F, we seek the best approximation which can not only supply accurate estimates of F at arbitrary locations on the domain, but will also provide accurate estimates of the partial derivatives and definite integrals of F anywhere on the domain. The domain of F will consist of points, $\{\mathbf{x}_k\}$, of arbitrary ordering and sub-clustering. A rectangular grid is a very special case of a data ordering.

Let us assume that an interpolation function, f, approximates F in the sense that

$$f(\mathbf{x}_k) = F(\mathbf{x}_k), \quad k = 1, 2, \ldots, N. \tag{1}$$

Given a finite number of data points, there is an infinite number of functions, f, which satisfy equation (1). There is no universally accepted "perfect" interpolating scheme, but we can restrict the class of interpolating functions to have certain desired properties. To restrict the class of functions we therefore require our "ideal" interpolating functions to be monotonic, i.e. not to introduce extraneous extrema, the interpolating functions to behave extremely accurately in flat as well as very steep regions, and to have very accurate estimates of derivative (partial derivatives) as well as definite integrals. We also expect the approximate interpolant to be robust; it should handle equally well any data arrangement and any surface shape. Finally, the "ideal" approximation shceme should be easily extended from one spatial dimension to two and three spatial dimensions.

2. SCATTERED DATA, GRID FREE APPROXIMATION SCHEMES

2.1. Discussion of polynomial methods

The oldest approximation scheme is an arbitrary polynomial expansion. This process will be briefly reviewed. Given N distinct points, $\mathbf{x}_k$, and values, F_k, there exists a unique polynomial, p_{N-1}, such that

$$p_{N-1}(\mathbf{x}_i) = F_i, \quad \text{for } i = 1, 2, \ldots, N. \tag{2}$$

Approximation processes may be local or global. Such a process which depends on data points in the immediate vicinity of a test point is called a local interpolation. One assumes that a local Taylor series expansion about the point, $\mathbf{x}_k$, is correct to a given order. On the other hand, the global approach assumes that the approximating function depends on all the data points. But the higher the order of a local interpolation, the more global it becomes because more data points are increasingly considered. For example, consider a scattered data set in two dimensions. A linear function requires at least three points, a quadratic function requires at least six points, a cubic requires at least 10 points, etc.

Local methods have been used extensively in numerical schemes for several reasons. First, the interpolant can be readily evaluated with a minimal amount of effort, and second, integral and derivative approximations are relatively simple to obtain, especially if the data points are equally spaced.

However, some of the drawbacks of the simple polynomial methods are: (1) polynomial snaking in higher order schemes which lead to poor derivative and integral estimates; (2) the lack of derivative continuity between consecutive local regions and (3) the slow convergence of low order polynomial approximations.

Splines are improvements to the local polynomial approach in that a local low order (typically cubic) fit is made over a local patch, but chosen in a manner that derivative continuity between local fits is guaranteed. Carlson and Fritsch [1, 2] have extended the spline technique further by imposing monotonicity constraints by controlling the derivative estimates. Hyman [3] and Dougherty *et al.* [4] also have investigated the cubic and quintic Hermite interpolations of Carlson and Fritsch. They have found that monotonicity and convexity constraints are important in converting an unacceptable interpolant into an excellent one.

Typically, the interpolation, derivative and integral estimate schemes which are based upon either polynomials, orthogonal polynomials or splines for higher spatial dimensions are formed as tensor products requiring a logically rectangular grid. Steep gradient regions can be treated by adaptive rectangular mesh refinement, see Berger and Oliger [5]. However, a logically rectangular mesh must be considered as a very restrictive type of data arrangement. In multidimensional Lagrangian and moving node fluid-dynamics, the original rectangular mesh usually tends to undergo a large amount of distortion. Low order interpolation techniques which are typically numerically diffusive are required to remap periodically the solution from the distorted grid onto a well-behaved rectangular grid.

Additional truncation error related problems occurring in fluid-dynamic simulations are the restrictions placed on zoning to minimize signal dispersion and true higher order transport, especially corner transport. van Leer [6] has devised one-dimensional transport schemes which

improve accuracy and noise reduction. A fully two-dimensional transport algorithm which is at least of second order accuracy is very desirable.

2.2. Review of scattered data interpolation techniques

Franke [7] recently published an extensive article which evaluated 29 different algorithms for the scattered data interpolation problem on a variety of known data surfaces. Franke graded various scattered data interpolation schemes according to the following criteria: accuracy, visual aspect, sensitivity to parameters, execution time, storage requirements and ease of implementation.

The methods he tested may be classified into the following groups: (1) inverse distance weighted methods; (2) rectangle based blending methods; (3) triangle based blending methods; (4) finite element based methods; (5) Foley's [8, 9] method and (6) global basis function methods. We shall summarize Franke's conclusions based on these methods.

The inverse distance weighting or Shepard's method was found to very dependent upon the weight function, and typically leaves flat spots at a data point. Rectangular based blending methods, although fast, performed rather poorly. Triangular based blending methods were found to have problems when long slim triangles are involved which are symptomatic of ill-conditioned Jacobians and give surfaces with errors.

In considering finite element based methods, Franke found that the C^1 (continuous first derivatives) based triangular elements were needed. However, very accurate estimates of the derivatives were necessary for both accuracy and the visual aspects of the surface. Again, poor results were due to long slim triangles. Franke claims such long slim triangles cannot be avoided without abandoning convexity or adding fictitious points.

Foley's [8, 9] method uses a generalized Newton type interpolant to generate a grid on which product type approximations can be constructed, An iterative correction is then made to the original approximation. The best performance of this scheme was found by using the generalized Newton interpolant with natural splines. In general, the surfaces were quite smooth, but sometimes exhibited polynomial-like "snaking" on the surfaces.

Of the class of methods tested, Franke found that global interpolation methods generally outperformed local interpolation methods. The principal disadvantage of global schemes is that the solution of set of N linear equations is required. The operation count increases at a rate of N^3 for such methods. Franke stated that of all the methods tested, Hardy's multiquadric method gave the most accurate results tested. The second best interpolation method was the thin-plate spline of Duchon [10, 11].

2.3. Review of the multiquadric (MQ) scheme and its development

Hardy [12, 13] first derived the two-dimensional multiquadric (MQ) scheme in 1968 to approximate geographical surfaces, and gravitational and magnetic anomalies. MQ was largely unknown to mathematicians until the publication of Franke's [7] review paper. Most mathematicians have not seriously studied this method because the mathematical analysis of MQ is very difficult, and it is not known why MQ performs so well (see Tarwater [14]).

Hardy's basic scheme is very simple and easy to implement. It is assumed that any function, f, may be written as an expansion of N continuously differentiable translates basis functions, g:

$$f(\mathbf{x}) = \sum_{j=1}^{N} a_j g_j(\mathbf{x} - \mathbf{x}_j), \tag{3}$$

where

$$g_j(\mathbf{x} - \mathbf{x}_j) = [d_j^2(\mathbf{x} - \mathbf{x}_j) + r^2]^{1/2}, \tag{4}$$

r^2 is a non-zero input parameter, and

$$d_j^2(\mathbf{x} - \mathbf{x}_j) = (x - x_j)^2 + (y + y_j)^2 + \cdots . \tag{5}$$

Another commonly used form of MQ's is the reciprocal multiquadric (RMQ) discussed by Hardy [12, 13], Frank [7] and Tarwater [14]. The RMQ basis function, h_j, is merely the reciprocal of equation (4)

$$h_j(\mathbf{x} - \mathbf{x}_j) = 1/g_j(\mathbf{x} - \mathbf{x}_j). \tag{6}$$

The coefficients, $\{a_j\}$ are found by solving a set of linear equations in terms of the basis functions. For example, for traditional MQ we solve

$$\sum_{j=1}^{N} a_j g_j(\mathbf{x}_i - \mathbf{x}_j) = F(\mathbf{x}_j), \quad i = 1, 2, \ldots, N \tag{7}$$

and $f(\mathbf{x}_i) = F(\mathbf{x}_i)$ which are given.

Micchelli's [15] theoretical investigations have proved that the MQ interpolation is always solvable for distinct data. He has shown that MQ coefficient matrix of rank N has one positive real eigenvalue and $(N - 1)$ negative real eigenvalues. Furthermore, he has shown that Duchon's thin plate spline is a positive definite interpolant which is related to Hardy's MQ interpolant which is conditionally positive definite [15]. The MQ interpolant can be positive definite by appending linear polynomials.

Franke [7] has found MQ performed better than RMQ. At first, this observation seems counter-intuitive since it diverges linearly with increasing distance. On the other hand, RMQ converges to zero as the reciprocal distance.

The asymptotic behavior of basis function of familiar expansions should guide us here in regarding MQ and RMQ bases functions. Legredre and Chebyshev functions are bounded in the interval $(-1, 1)$. Laguerre and Hermite bases function of nth order diverge as x^n in the intervals $(0, \infty)$ and $(-\infty, \infty)$, respectively, see Ref. [16]. The behavior of a function expanded in terms of the latter two basis functions in the asymptotic region is governed by the expansion coefficients. Note we demand that the weighted integral of the square of the basis functins over their respective domains must exist. The existence of similar integrals for the MQ basis functions will be discussed later.

Tarwater [14] investigated MQ to determine the effect of varying the parameter, r^2, on the goodness of fit. Various experiments were tried to obtain increasingly more accurate interpolants. It was found that the r.m.s. error was a function of the magnitude of r^2; for increasing r^2, the errors dropped to a minimum called the optimum r^2, and grew rapidly thereafter. She showed that for the several problems examined, the r.m.s. errors of the MQ interpolation compared favorably or even outperforms the monotonic cubic spline for accuracy. By adjusting the parameter r^2, she found that the accuracy could be considerably improved. The most difficult function to interpolate was the steep "cliff" function. She suggested that the shape of the surface to be fitted is a factor in optimizing the accuracy. Lancaster and Salkauskas [17] also noted that noisy surfaces correspond to the ill-conditioning of the MQ coefficient matrix can occur if r becomes large.

Stead [18], like Franke [7], examined various methods for estimating partial derivatives on scattered data. She concluded that for surfaces with large curvature, MQ is excellent for obtaining very accurate derivative estimates, but that MQ behaves poorly on relatively flat surfaces. She therefore recommended a combination of techniques in which MQ would be applied to steep surfaces and a quadratic fit would be used for relatively flat surfaces without using transformations such as stretching functions which causes a change in geometry.

2.4. Recent improvements to MQs

In the effort to push the accuracy of MQ, we found MQ can be made exceptionally accurate by carefully modifying the scheme in such a way that MQ coefficient matrix is well-conditioned. We simultaneously improved the accuracy and reduced the condition number by permitting the parameter r^2 to vary, thus giving rise to nearly flat sheet-like functions to very narrow cones. When necessary, we transformed the original data set to appear more scattered to reduce the condition number. Thirdly, and most importantly, we improve accuracy and reduce dramatically the computational effort by transforming a large global problem into many small quasi-local problems by domain decomposition.

We found that surfaces could be approximated to a very high degree of accuracy by permitting r^2 to vary with basis function number. The value of r^2 controlled the shape of the basis function. large r^2 values gave rise to flat sheet-like basis functions, intermediate r^2 values gave rise to bowl-like basis functions; small r^2 values gave rise to narrow cone-like basis functions. By adding and subtracting a diverse collection of different shaped basis functions, very accurate results have been obtained.

The key factor in obtaining accurate results was the conditioning of the MQ coefficient matrix. The more distinct are the entries of a full matrix, the lower is it condition number. Therefore, we permit only a monotonic variation of r^2. We have found no significant changes in accuracy whether the r^2 variation was monotonically increasing or decreasing with the basis function number, j. In addition, a random permutation of the r^2 parameter seemed to have little effect. Both linear and exponential variation worked very well, but exponential variations gave a better conditioned coefficient matrix:

$$r^2(j) = r^2 \min(r^2_{\max}/r^2_{\min})^{(j-1)/(N-1)}, \quad j = 1, 2, \ldots, N, \tag{8}$$

and r max^2 and r min^2 are input parameters. Using equations (3)–(5) and (9), the MQ expansion is given as

$$f(\mathbf{x}) = \sum_{j=1}^{N} a_j[d^2(\mathbf{x} - \mathbf{x}_j) + r^2(j)]^{1/2}. \tag{9}$$

Our numerical observations show that the more distinct the entries of the MQ coefficient matrix are, the lower MQ coefficient matrix condition number becomes, and the better is the accuracy. However, a wide variation in r^2 is not sufficient for high accuracy because the MQ basis functions also depend on distances.

As with Foley [20], we observed that performance of MQ was sensitive to scaling. That is, it was important to the condition number whether distances were expressed in centimeters or meters. Likewise, Tarwater [14] and Foley [20] have shown that "track data", i.e. data which is closely spaced along one coordinate direction, and widely spaced along the orthogonal direction, gives MQ interpolants with very large errors.

For consistent results, regardless of scale problems or track data problems, all data, even using subdomain decomposition, were mapped onto a unit line for one-dimensional problems and onto a unit square for two-dimensional problems. If three or more distance pairs on the unit square are nearly degenerate, then additional transformations are undertaken to deliberately make the transformed distances more distinct. We shall discuss this strategy when discussing an example problem.

To summarize, two concurrent strategies were undertaken to obtain very accurate MQ results. First, we allowed the r^2 parameter to vary with basis function number allowing very flat to very conical shaped basis functions to represent the surface. Second, we scaled the independent coordinates to unity, and then introduced additional rotations and shear transformations to make the distance pairs sufficiently distinct, if necessary.

The accuracy of the interpolants, partial derivative estimates and definite integrals is influenced by the condition number of the matrix and the gradients of the surface. In contrast to ordinary polynomial based methods of a prescribed order, we observed that MQ is increasingly more accurate on steeper gradient surfaces with respect to analytic functions. The flat or gentle gradient surfaces are somewhat noisy with MQ with respect to analytic functions.

The apparent reason why MQ is noisy on flat surfaces, and elsewhere is as follows. Flat surfaces are represented by linear combinations of very large r^2 basis functions. But as $r^2(j)$ become large, so does the condition number. The resulting coefficients are very large in magnitude and vary in sign. On a computer with a finite word representation, the lack of word precision gives noisy results in flat regions, but excellent results in regions with modest to large gradients which are well-approximated by basis functions with small to intermediate values of r^2. There does not appear to be any theoretical limit to MQ, but rather an implementation limit in shallow gradient regions which are handled excellently by traditional methods such as monotonic cubic splines [1, 2].

We performed an eigenvalue analysis on the non-symmetric MQ coefficient matrices, see equations (8) and (9). These matrices are typical of those problems presented in the next section.

The results were similar to those reported by Micchelli [15] using the symmetric form. If the condition number of the coefficient matrix is within machine precision limits, then there is one large positive real eigenvalue; the remaining eigenvalues are real and negative. As the condition number is increased by increasing the magnitude of the r^2 parameters, the behavior is essentially the same as before, but very small complex eigenvalues appear in pairs.

Another very important consideration for accuracy is the number of data points fitted. The larger the coefficient matrix, the larger its condition number becomes. It was very important to partition a domain into several subdomains for better accuracy, computational efficiency. For these surface with sufficiently non-zero gradients, the examples to be presented in the Results section are generally accurate from 6 to 10 significant digits of accuracy. In the common overlap regions between two subdomains, the fitted functions from either region have the same functional value at the data locations, but have different values in between. Hence the approximants could be mismatched away from data points. We could have calculated the partial derivatives at the data locations in common from the function in one subdomain, and required that the approximating function in the next subdomain sharing the common data points not only have the same functional values, but also the same partial derivatives, see equation (8). A few iterations over all the subdomains would insure that the approximations are C^1 continuous. This was found to be unnecessary since the approximants were mismatched in the 6–8th significant figure. So all appropriate quantities were blended by using weighted averages in the common overlapping regions. Although this simple blending scheme worked well in our studies, Franke's scheme is recommended since it guarantees continuity.

Franke [21] has also discussed the process of blending approximants across overlapping subdomains to achieve a continuous surface using the method of Schiro and Williams [22]. This was done via Hermite cubics. The MQ method was used to fit the differences, data minus mean value, and this was observed to have a beneficial effect on the magnitude of the coefficients. Damon [23] also blended surfaces constructed from subdomain decomposition using the method of weighted averages.

As stated previously, we observed that MQ is excellent in regions whose surfaces have gradients that are not too small. In thse regions, MQ is very accurate, convex and monotonic as observed in our computer experiments. Relatively shallow gradients can be treated by first applying a transformation to steepen the gradients, solving for the coefficients, interpolating or differentiating and then applying the inverse transformation. However, this steepening technique is not sufficiently general. We will recommend a hybrid scheme which is general and uses monotonic polynomials in relatively flat regions and MQ elsewhere.

3. SOME JUSTIFICATIONS FOR THE SUCCESS OF THE HARDY MQ SCHEME

Tarwater [14] stated that Hardy's MQ scheme has not been seriously studied by mathematicians other than Micchelli [15] because "its analysis is very difficult". Of the scattered data schemes, only the simplest form of local triangular interpolation has been analyzed. Foley [24] derived error bounds of his multistage methods which depends on h, the maximum distance from the nearest data point. This section will review the latest developments in the theory of MQ since Tarwater's work.

Hardy and Nelson [25] have given a physical reason why MQ performs so well. If we regard a surface or body to be generated by a potential function which satisfies Laplace's equation, such harmonic functions share a common difficulty. These potentials have singularities at the source point and cannot be easily evaluated at or near sources which induce the potential. They have found an alternative form for representing a disturbing potential which is biharmonic in nature and which can be used for evaluations at points collocated with sources. Although the MQ basis functions are unbounded at infinity, they have shown that the potential function vanishes at infinity only if the sum of the expansion coefficients vanishes.

Hardy [26] showed that MQ is an appropriate approximation to biharmonic representations and RMQ is the appropriate approximation to a harmonic representation of the disturbing potential. Thus the multiquadric–biharmonic representations and approximations have the advantage over other methods since data points do not need to be separated from source points.

Another explanation of why MQ works so well will be advanced here. The best MQ results were found to occur for large variations of r^2 terms which give large variations in the coefficient matrix. Given that $\{d_j^2\}_{\max} < \{r_j^2\}_{\min}$, then the following infinite Taylor series expansion holds over the N data points:

$$f(\mathbf{x}) = \sum_{j=1}^{N} a_j r(j) \left[\sum_{m=0}^{\infty} [(dj)/r(j)]^{2m}/(2^m m!) \prod_{k=0}^{m-1} (1-2k) \right], \tag{10}$$

where $d(j) = [(x - x_j)^2 + (y - y_j)^2 + \cdots]^{1/2}$. A similar series expansion exists for the asymptotic region where $\{r_j^2\}_{\max} < \{d_j^2\}_{\min}$.

The MQ Taylor series expansions, equation (10), is an infinite order expansion of all even terms of the distances, d_j. Unlike the finite polynomial expansions, the MQ expansion is an infinite order multivariant polynomial expansion in terms of a finite number of data points. Because r^2 can vary many orders of magnitude, the effective expansion is very high order up to the remaining terms which have become truncated in a finite precision computer. Furthermore, unlike the tensor product formulations, the MQ expansions contain contributions from not only the direct terms, but all cross product contributions. Since the $r(j)$ terms differ vastly by orders of magnitude, the contributions range from locally constant to very high order multivariate polynomial expansions.

Madych and Nelson [27] consider a general class of interpolants which includes a polynomial of degree less than some fixed integer m given by

$$f(\mathbf{x}) = \sum_{n=1}^{N} a_j g(\mathbf{x} - \mathbf{x}_j) + \sum_{|\alpha| < m} k_\alpha \mathbf{x}^\alpha, \tag{11}$$

where a_j and k_α must satisfy

$$\sum_{j=1}^{N} a_j g(\mathbf{x}_i - \mathbf{x}_j) + \sum_{|\alpha| < m} k_\alpha \mathbf{x}_i^\alpha = f_i(\mathbf{x}_i) = F_i, \quad i = \{1, 2, \ldots, N\}, \tag{12a}$$

$$\sum_{j=1}^{N} a_j \mathbf{x}_j^\alpha = 0, \quad |\alpha| < m. \tag{12b}$$

A sufficient condition which makes equation (11) solvable for all f, is that g be conditionally positive definite

$$\sum_{i,j=1}^{N} \bar{a}_i a_j g(\mathbf{x}_i - \mathbf{x}_j) \geqslant 0, \tag{13}$$

for all distinct points $\mathbf{x}_1, \mathbf{x}_2, \ldots, \mathbf{x}_N$ in R^n, and for all complex number $a_i \neq 0$ satisfying equation (12b). The class of all conditionally positive definite functions of order m on R^n is denoted as Q_m.

They have shown for distinct points, $\mathbf{x}_1, \ldots, \mathbf{x}_N$ satisfying the interpolation problem, equation (11), and for the class of interpolants in Q_m satisfying equation (13), that a semi-norm exists which is minimized by such interpolants. They show that the following functions are conditionally positive definite:

$$h(\mathbf{x}) = 1 + c|\mathbf{x}|^2)^{(2k+1)/2}, \quad \text{for } k = -1, 0, 1, 2, \ldots, \quad \text{(generalized MQ)} \tag{14}$$

$$h(\mathbf{x}) = (-1)^{k+1}(1 + c|\mathbf{x}|^2)^k \log(1 + c|\mathbf{x}|^2), \quad \text{(Duchon's thin plate splines)} \tag{15}$$

$$h(x) = \exp(-c|\mathbf{x}|^2), \quad \text{(rotating Gaussians)} \tag{16}$$

for all $c > 0$.

Further, many types of interpolation conditions are allowed such as derivatives and integrals of the interpolating functions.

4. COMPUTATIONAL RESULTS

In this section, we shall present the results of the basis MQ scheme applied to a suite of problems. Among the application whose reuslts will be examined are:

1. The two-dimensional interpolation from a coarse regular grid onto a finer regular grid. One immediate application of this problem is in mesh refinement and dynamic multigrid methods.
2. The two-dimensional interpolation from a scattered data set onto a fine regular grid.
3. Two-dimensional derivative estimates of functions over a regular grid and an arbitrary data set.
4. Two-dimensional interpolation over a scattered data set using the Madych–Nelson MQ approximation.
5. The dynamic arbitrary Lagrangian–Eulerian (ALE) remapping procedure used in Lagrangian fluid dynamics codes.

In each example, domain decomposition was used. Subsets of 16–25 points were partitioned from the domain of all independent positions. To ensure continuity of the function and its derivatives at the subdomains, overlapping contiguous neighboring subdomains were constructed so the method of weighted averages could blend the solutions over the overlapping subset regions.

4.1. Two-dimensional interpolation from a coarse grid onto a fine grid

Two test functions, $f_1 = \exp(2x + 3y)$ and $f_2 = \exp[-(2x + 3y)^2]$ were evaluated on the vertices of a uniform 5×5 grid, see grid A, Fig. 1. There were 36 values of each function stored at these vertices.

The domain was decomposed into two overlapping subdomains containing 24 points each. The first subdomain contained 24 points from points 1–24 where the first point is on the lower left hand corner. The numbering is ordered by rows. The second subdomain contained 24 points from points 18–36.

We note that the MQ coefficient matrix and its inverse are independent of the function. The expansion coefficients for each function on each subdomain were calculated and stored. Then the interpolated function was calculated on grid B. There were a total of 96 interpolants.

The overlap regions which contain the results of the interpolants from the two subdomains were blended by the method of weighted averages. The results of the interpolated results for function f_1 is given in Table 1. Table 2 gives the exact results calculated at the same positions. The results in Table 1 are remarkably close. However, the interpolants of f_2 were poor and noisy. The reason for this poor behavior is that function f_2 becomes flat very rapidly away from the point $(0, 0)$.

Experience has shown MQ appears to be excellent on shallow to steep gradient surfaces. Therefore we formed a new function, $1/f_2$. The expansion coefficients were formed using the inverse

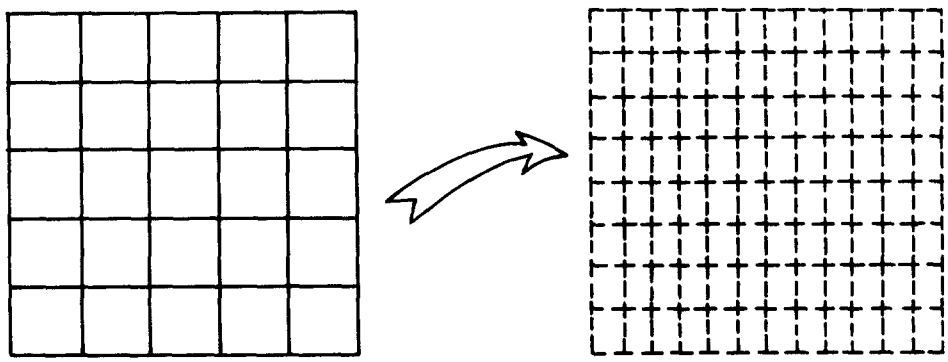

Fig. 1. Interpolation of functions from a coarse grid onto a finer grid.

Table 1. Interpolation of $\exp(2x + 3y)$ over grid B

1.000000	1.054041	1.111003	1.171043
1.234328	1.301032	1.371342	1.445451
1.523564	1.605900	1.692685	1.784159
1.880578	1.982206	2.089327	2.202237
2.321249	2.446692	2.578914	2.718282
2.865181	3.020019	3.183225	3.355250
3.536572	3.727693	3.929142	4.141478
4.365288	4.601194	4.849848	5.111940
5.388195	5.679380	5.986301	6.309808
6.650798	7.010215	7.389056	7.788370
8.209263	8.652902	9.120515	9.613399
10.13292	10.68051	11.25770	11.86608
12.50734	13.18325	13.89569	14.64663
15.43816	16.27245	17.15184	18.07874
19.05574	20.08554	21.17098	22.31509
23.52103	24.79213	26.13193	27.54413
29.03265	30.60191	32.25536	33.99848
35.83580	37.77214	39.81368	41.96526
44.23311	46.62353	49.14312	51.79887
54.59815	57.54870	60.65871	63.93678
67.39200	71.03395	74.87271	78.91890
83.18379	87.67916	92.41743	97.41179
102.6760	108.2248	114.0733	120.2380
126.7359	133.5849	140.8039	148.4132

Table 2. Exact solution of $\exp(2x + 3y)$ over grid B

1.000000	1.054041	1.111003	1.171043
1.234328	1.301032	1.371342	1.445451
1.523564	1.605900	1.692685	1.784159
1.880578	1.982206	2.089327	2.202237
2.321249	2.446692	2.578914	2.718282
2.865181	3.020019	3.183225	3.355250
3.536572	3.727693	3.929142	4.141478
4.365288	4.601194	4.849848	5.111940
5.388195	5.679380	5.986301	6.309808
6.650798	7.010215	7.389056	7.788370
8.209263	8.652902	9.120515	9.613399
10.13292	10.68051	11.25778	11.86608
12.50734	13.18325	13.89569	14.64663
15.43816	16.27245	17.15184	18.07874
19.05574	20.08554	21.17098	22.31509
23.52103	24.79213	26.13193	27.54413
29.03265	30.60161	32.25536	30.99848
35.83580	37.77241	39.81368	41.96526
44.23311	46.62353	49.14312	51.79887
54.59815	57.54870	60.65871	63.93678
67.39200	71.03395	74.87271	78.91892
83.18380	87.67916	92.41745	97.41180
102.6761	108.2248	114.0734	120.2381
126.7359	133.5858	140.8039	148.4132

in each subdomain, and interpolated onto the fine grid. Afterwards, the inverse of the inverse which is f_2 was taken again and presented on Table 3. The exact solution at the same locations is presented in Table 4.

4.2. Two-dimensional interpolation from a scattered data set using domain decomposition onto a very fine regular grid

The next set of experiments deal with the scattered data problem. Figure 2 shows the x–y data distribution on a unit square containing 60 points. The domain of 60 points was decomposed into patches each containing a minimum of 16 points. Some of the points may be contained in the overlap of previous patches. Because smaller systems of equations were involved in finding the expansion coefficients and the distances are more scattered, the numerical results were even better than the previous examples. Accuracy from 7 to 10 significant digits was obtained. There is no visual difference between the plots of the exact solution and the MQ generated solution. Our results in these problems are better than the previous examples becuase 60 data points rather then 36 were used to define the initial distribution. Franke [7] also showed that his test functions were better with 100 points than with 33 or 25 points, since the denser point set gave more sample points to be fitted.

Table 3. MQ interpolation of exp[−(2x − 3y)**2]over grid B

1.0000	0.99723	0.98898	0.97538
0.95665	0.93309	0.90509	0.87307
0.83754	0.79901	0.75805	0.71521
0.67106	0.62616	0.58104	0.53619
0.49207	0.44908	0.40758	0.36788
0.33021	0.29476	0.26166	0.23099
0.20279	0.17705	0.15373	0.13274
0.11398	9.73308e − 02	8.26554e − 02	6.98050e − 02
5.86268e − 02	4.89664e − 02	4.06718e − 02	3.35958e − 02
2.75976e − 02	2.25450e − 02	1.83157e − 02	1.47975e − 02
1.18891e − 02	9.49949e − 02	7.54831e − 02	5.96480e − 02
4.68744e − 03	3.66324e − 03	2.84698e − 03	2.20037e − 03
1.69124e − 03	1.29276e − 03	9.82720e − 04	7.42896e − 04
5.58480e − 04	4.17519e − 04	3.10420e − 04	2.29524e − 04
1.68767e − 04	1.23397e − 04	8.97280e − 05	6.49010e − 05
4.66970e − 05	3.34066e − 05	2.37487e − 05	1.67836e − 05
1.18056e − 05	8.26427e − 06	5.74577e − 06	3.96694e − 06
2.72960e − 06	1.87355e − 06	1.27624e − 06	8.61616e − 07
5.79948e − 07	3.89907e − 07	2.60327e − 07	1.71518e − 07
1.12087e − 07	7.39608e − 08	4.85813e − 08	3.06182e − 08
1.95095e − 08	1.29288e − 08	8.08278e − 09	4.82781e − 09
3.16772e − 09	2.06205e − 09	1.14387e − 09	7.19099e − 10
4.89659e − 10	2.64501e − 10	1.54074e − 10	1.05250e − 10
6.08194e − 11	3.16446e − 11	2.09348e − 11	1.38879e − 11

Table 4. Exact solution of exp[(−(2x + 3y)**2] over grid B

1.0000	0.99723	0.98898	0.97538
0.95665	0.93309	0.90509	0.87307
0.83754	0.79901	0.75805	0.71521
0.67106	0.62616	0.58104	0.53619
0.49207	0.44908	0.40758	0.36788
0.33021	0.29476	0.26166	0.23099
0.20279	0.17705	0.15373	0.13274
0.11398	9.73308e − 02	8.26554e − 02	6.98050e − 02
5.86267e − 02	4.89664e − 03	4.06720e − 03	3.35959e − 03
2.75976e − 02	2.25450e − 02	1.83156e − 02	1.47975e − 02
1.18891e − 02	9.49956e − 03	7.54835e − 03	5.96478e − 03
4.68738e − 03	3.66320e − 03	2.84698e − 03	2.20041e − 03
1.69128e − 03	1.29277e − 03	9.82699e − 04	7.42872e − 04
5.58473e − 04	4.17526e − 04	3.10427e − 04	2.29524e − 04
1.68769e − 04	1.23410e − 04	8.97431e − 05	6.49002e − 05
4.66751e − 05	3.33825e − 05	2.37436e − 05	1.67945e − 05
1.18136e − 05	8.26401e − 06	5.74902e − 06	3.97732e − 06
2.73641e − 06	1.87226e − 06	1.27393e − 06	8.62019e − 07
5.80074e − 07	3.88189e − 07	2.58344e − 07	1.70980e − 07
1.12535e − 07	7.36588e − 08	4.79462e − 08	3.10369e − 08
1.99800e − 08	1.27911e − 08	8.14356e − 09	5.15601e − 09
3.24644e − 09	2.03280e − 09	1.26583e − 09	5.15601e − 10
4.82749e − 10	2.95655e − 10	1.80070e − 10	7.83885e − 10
6.56960e − 11	3.93530e − 11	2.34429e − 11	1.38879e − 11

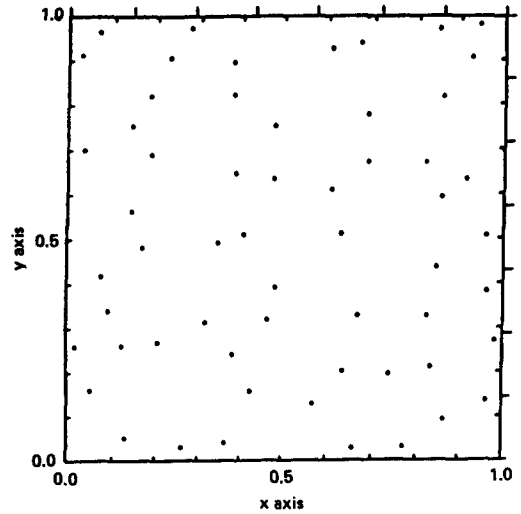

Fig. 2. Plot of 60 scattered data points over a unit square.

The following two-dimensional functions, f_3–f_6, inclusively, were used as input at the location positions shown in Fig. 2. These functions are:

$$f_3 = 9\begin{cases} 0.75\exp[-(x-3)^2/4 - (y-3)^2/4] + 0.75\exp(-x/49 - y/100) & (17) \\ -0.75\exp[-(x-3)^2/4 - (y-4)^2/4] - 0.2\exp[-(x-5)^2 - (y-8)^2] \end{cases}, \quad (18)$$

$$f_4 = \exp[-9(x-0.5)^2 - 9(y-0.25)^2], \quad (19)$$

$$f_5 = \cosh(x-0.5)\cosh(y-0.5), \quad (20)$$

$$f_6 = 2x + 3y. \quad (21)$$

The x, y data set of 60 points were scattered on the space $[0, 1] \times [0. 1]$. At these locations, the exact quantities $f(x_i, y_i)$ were calculated and stored. The same x, y data set was used in each of the surfaces to be presented. Starting from a corner, a domain of 16 x, y points was chosen, fitted by MQ, and interpolated onto a new mesh of 1225 points consisting of 35 points in both the x and y directions. The exact surface and the MQ surface are indistinguishable from one another, see Figs 3–6.

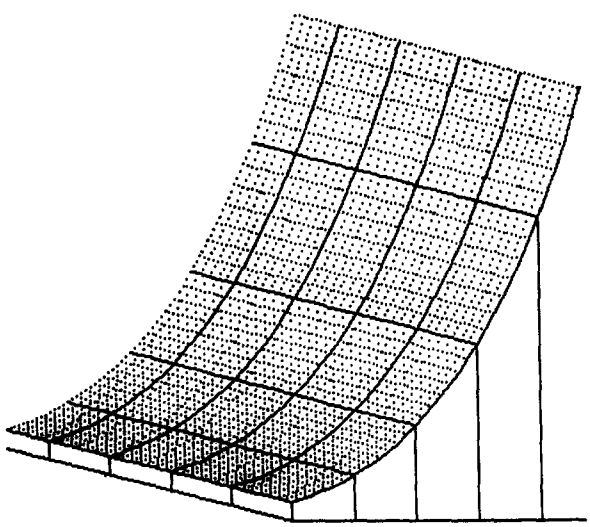

Fig. 3. MQ fit of functions f_3 from a scattered data distribution onto a 35 × 35 fine grid.

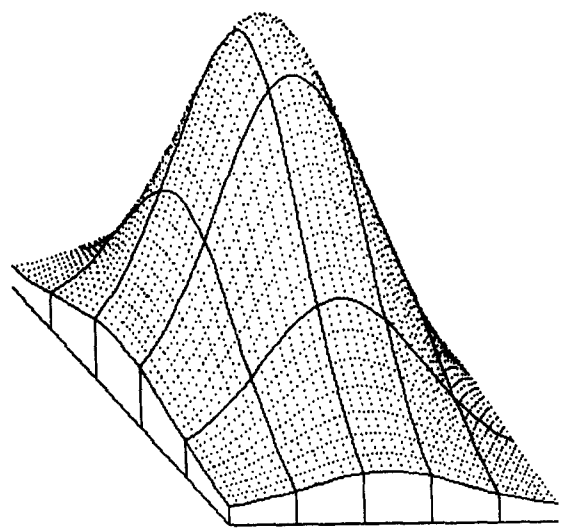

Fig. 4. MQ fit of function f_4 from a scattered data distribution onto a 35 × 35 fine grid.

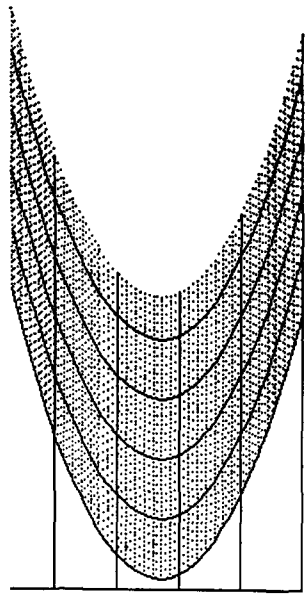

Fig. 5. MQ fit of function f_5 from a scattered data distribution onto a 35 × 35 fine grid.

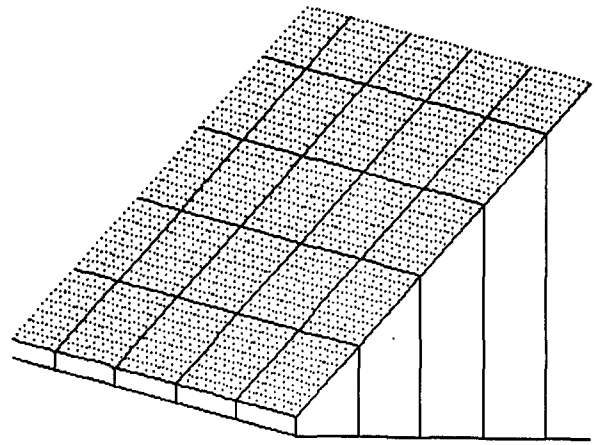

Fig. 6. MQ fit of function f_6 from a scattered data distribution onto a 35 × 35 fine grid.

4.3. Partial derivative estimates obtained form two-dimensional regular and scattered data

In this subsection, we shall present the results of partial derivative estimates obtained from functions f_1–f_6, inclusively. In some instances we chose locations at which these functions had local extrema. Because of machine round-off, the MQ estimates were not exactly zero, but tended to be less than 10^{-7} in magnitude. We shall denote the MQ zero as 0.0*. Other examples of derivative calculations are found in Ref. [19].

For convenience, we shall present in tabular form the derivative estimates of these functions at three different spatial locations: (0, 0), (1/4, 1/2) and (1/2, 1/2) in Tables 5–7. As we will show, the derivative estimates as well as interpolations are excellent in regions with modest to very steep gradients.

4.4. Results with the Madych–Nelson MQ scheme

In our previous investigations using only the expansion of MQ basis functions, we found that such function approximations are excellent in regions which have moderate to steep gradients. In an effort to generalize MQ, we used Madych and Nelson's generalization [27], see equation (11) and appended a constant to the MQ expansion yielding

$$f(\mathbf{x}) = k_0 + \sum_{j=2}^{N} a_j[g(\mathbf{x} - \mathbf{x}_j) - g(\mathbf{x} - \mathbf{x}_l)]. \tag{22}$$

We investigated the goodness of five functions using the scattered data configuration shown in Fig. 2. These functions are

$$f_7(x, y) = [5/4 + \cos(5.4y)]/[6 + 6(3x - 1)^2], \tag{23}$$

$$f_8(x, y) = \{64 - 81[(x - 1/2)^2 + (y - 1/2)^2]\}^{1/2}/9 - 1/2, \tag{24}$$

$$f_9(x, y) = \exp\{-(81/16)[(x - 1/2)^2 + (y - 1/2)^2]\}/3, \tag{25}$$

Table 5. Location (0, 0)

Function	MQ ($\partial f_i/\partial x$)	Exact ($\partial f_i/\partial x$)	MQ ($\partial f_i/\partial y$)	Exact ($\partial f_i/\partial y$)
1	1.9999	2.0000	3.0000	3.0000
2	0.0*	0.0000	0.0*	0.0000
3	−330.65	−330.65	0.276	0.0276
4	0.0998	0.0998	0.0998	0.0998
5	−0.5875	−0.5876	0.0*	0.0000
6	2.0000	2.0000	3.0000	3.0000

Table 6. Location (1/4, 1/2)

Function	MQ ($\partial f_i/\partial x$)	Exact ($\partial f_i/\partial x$)	MQ ($\partial f_i/\partial y$)	MQ ($\partial f_i/\partial y$)
1	14.778	14.778	22.167	22.167
2	−0.1465	−0.1465	−0.2198	−0.2198
3	−327.18	−327.18	0.1446	0.1446
4	2.5640	2.5640	0.0*	0.0000
5	−0.2605	−0.2605	−0.2605	−0.2605
6	2.0000	2.0000	3.0000	3.0000

$$f_{10}(x, y) = \exp\{-(81/4)[(x - 1/2)^2 + y - 1/2)^2]\}/3, \tag{26}$$

$$f_{11}(x, y) = 1 + \tanh(9y + 9x). \tag{27}$$

Table 8 shows the l_2 and l_∞ norm errors for the interpolants using equation (22) over a 35 × 35 (1225) refined grid. The definition of l_2 error used is

$$\sum_{i=1}^{N} (z_i^{\mathrm{MQ}} - z_i^{\mathrm{exact}})^{1/2}/N.$$

We see that equation (22) (MQ expansion with an appended constant) gives very good approximations as long as we have no flat regions. Functions f_{10} and f_{11} are much improved using equation (22) rather than equation (9), but the fact is that such approximations are slightly non-monotonic in flat regions.

We attempted to improve the approximation to function f_{11} by appending a linear polynomial to the MQ expansion. The results were disappointing in that the max error increased by a factor of 20 over the results in Table 8.

These experiments show that MQ or MQ with an appended constant give excellent results for regions with moderate to steep gradients where traditional polynomial expansions fail. But MQ performed poorly on flat regions where traditional methods work well. Our strategy will be to use a hybrid scheme over all cases.

4.5. Dynamic ALE Remapping of the two-dimensional Blake problem

Figure 7 illustrates the setup of the Blake problem [28]. The solid wedge is composed of an elastic solid whose density is 2000.00. At the bottom boundary a pressure pulse is applied for a duration of $3.873 \cdot 10^{-5}$. Profiles will be presented along the dashed line AB.

The objective of this exercise is to freeze the solid time-marching fluid dynamics, but permit the underlying mesh to move. In the ideal case, the surfaces of the dependent variables are independent and invariant under changes of the underlying mesh.

Figure 8 shows the mesh as it evolves during the ALE remapping. The middle mesh has opened to its greatest extent after 180 ALE cycles. The lower mesh closes back to the original configuration after a total of 360 ALE cycles.

Figures 9–12 show the internal energy, solid density and pressure at 0, 180 and 360 ALE cycles. Both the contours and the profiles at the line AB of Fig. 7 are displayed.

The computational domain was subdivided into 15 patches to find the two-dimensional density, pressure and internal energy surface on the next mesh increment configuration. Because MQ is not accurate in very flat regions, the calculations reverted to a quadratic approximation if the $(z \max - z \min) < 0.05$ within a patch. The parameters for r^2 were preset, and the local patch coefficient matrix condition number was kept within prescribed bounds by scaling the r^2 column variation. The remapping process is totally conservative whether the interpolation process is done by a first order interpolation or by MQ interpolation. The sum of all the masses in the zones was found to be a constant at all stages of the remapping process. The matrix inverse was found on

Table 7. Location (1/2, 1/2)

Function	MQ ($\partial f_i/\partial x$)	Exact ($\partial f_i/\partial x$)	MQ ($\partial f_i/\partial y$)	Exact ($\partial f_i/\partial y$)
1	24.365	24.365	36.547	36.547
2	−0.0192	−0.0193	−0.2895	−0.2895
3	−325.44	−325.44	0.2771	0.2270
4	0.0*	0.0000	0.00001	0.0000
5	0.0*	0.0000	0.0*	0.0000
6	2.0000	2.0000	3.0000	3.0000

Table 8. The l_2 and l_∞ errors for functions f_7–f_{11} using equation (22) as the approximation

Function	l_2 norm error	l_∞ norm error
f_7	$4 \cdot 10^{-7}$	$1 \cdot 10^{-4}$
f_8	$1 \cdot 10^{-9}$	$8 \cdot 10^{-7}$
f_9	$1 \cdot 10^{-9}$	$6 \cdot 10^{-7}$
f_{10}	$6 \cdot 10^{-7}$	$6 \cdot 10^{-4}$
f_{11}	$3 \cdot 10^{-5}$	$1 \cdot 10^{-2}$

a sub-domain. All other coefficients of the dependent variable expansion coefficients were found by a simple matrix–vector multiply.

The higher order ALE scheme using MQ as the interpolant was implemented in an existing two-dimensional code. At each ALE cycle in which a new mesh is formed from an old mesh, six ALE sybcycles were used. At each subcycle, alternating sets of nodes were moved to the new locations so that the overlap between the old and new partial mesh form triangles. At each subcycle, MQ is used as the interpolant, and the appropriate densities were interpolated at the centroids of the triangles, and integrated. The integrated quantities were added to the new mesh and subtracted from the old mesh insuring rigorous conservation. The relaxation subcycling continued until all nodes were moved to the new mesh location. Thus MQ was applied in this remapping problem a total of 2160 times during the 360 ALE cycles.

We note that the MQ interpolation scheme preserved the basic shape of the surface even after 180 and 360 ALE cycles, except for some distortion in the flat tail region.

Dukowicz and Kodis [29] have recently developed second order accurate, conservative rezoning scheme for ALE computations. They assumed that the density distribution within each cell is linear, and limited the gradients to preserve monotonicity. They have emphasized the need for the interpolation process to be monotonic and conservative so that no non-physical negative densities or energies are created in the remapping process.

As demonstrated, the application of the ALE technique is both conservative and monotonic when MQ is the interpolant. Furthermore, MQ preserves the proper symmetry at the boundaries of the pie-shaped mesh. After 360 ALE remaps, the original contour and profiles are very well-preserved.

We note that the zone center in this ALE remapping problem, see Fig. 8, appears to behave very similarly to the "track" data problem described by Tarwater [14] and Foley [20]. Track data are data which are closely spaced along one coordinate axis, and which are widely spaced along another coordinate axis. Note, in Fig. 8, that the zones especially at 180 ALE cycles have very poor aspect ratios.

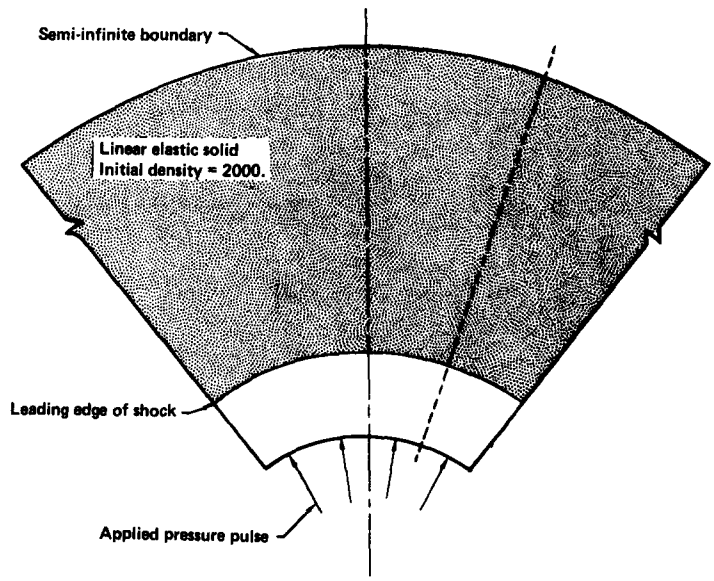

Fig. 7. Schematic of Blake's problem. A pressure pulse applied to a linear elastic solid.

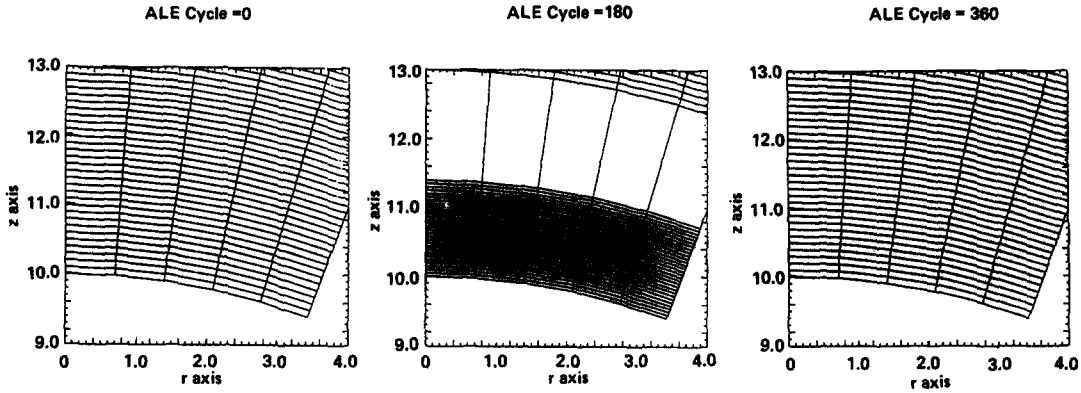

Fig. 8. Distortion of a cylindrically symmetric mesh as it undergoes mesh distortion.

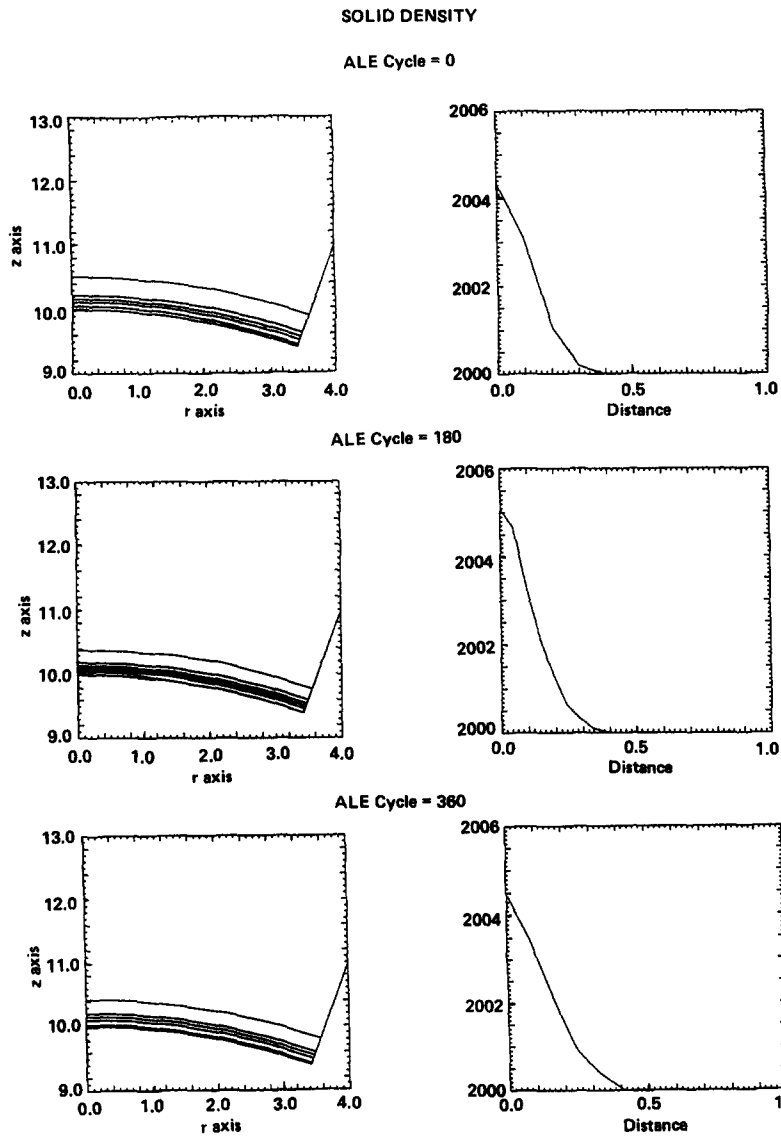

Fig. 9. Contour and profile plots of the solid density at 0, 180 and 360 major ALE cycles.

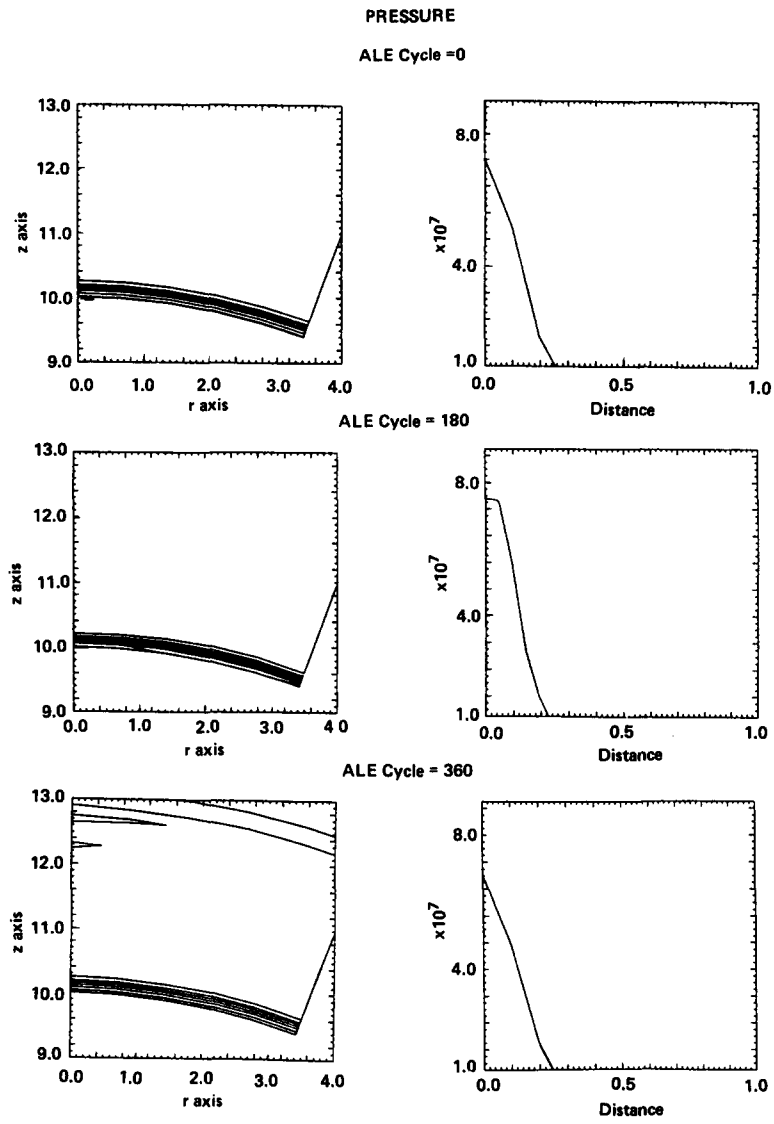

Fig. 10. Contour and profile plots of the solid pressure at 0, 180 and 360 major ALE cycles.

We have conjectured that the reason why "track" data does not yield accurate MQ approximates is that too many of the distances in the MQ expansion are similar. We counteracted the "track" data problem by introducing a transformed coordinate system in which the transformed distances appeared to be uniformly scattered. This was done by scaling, rotating and adding shear terms.

We first found $\min(x_i - x_j)$ and $\min(y_i - y_j)$, $i \neq j$, and introduced new independent variables for each data point i:

$$\begin{aligned} s_j &= (x - x_y)/\min(x_i - x_j), && i \neq j, \\ &= 0, && \iota = j \end{aligned} \tag{28}$$

$$\begin{aligned} t_j &= (y - y_j)/\min(y_i - y_j), && i \neq j, \\ &= 0 && i = j. \end{aligned} \tag{29}$$

Next, we introduced shear transformations of the form

$$u_j = \alpha s_j + \beta t_j + \gamma s_j t_j, \tag{30}$$

$$v_j = \delta s_j + \epsilon t_j + \phi s_j t_j, \tag{31}$$

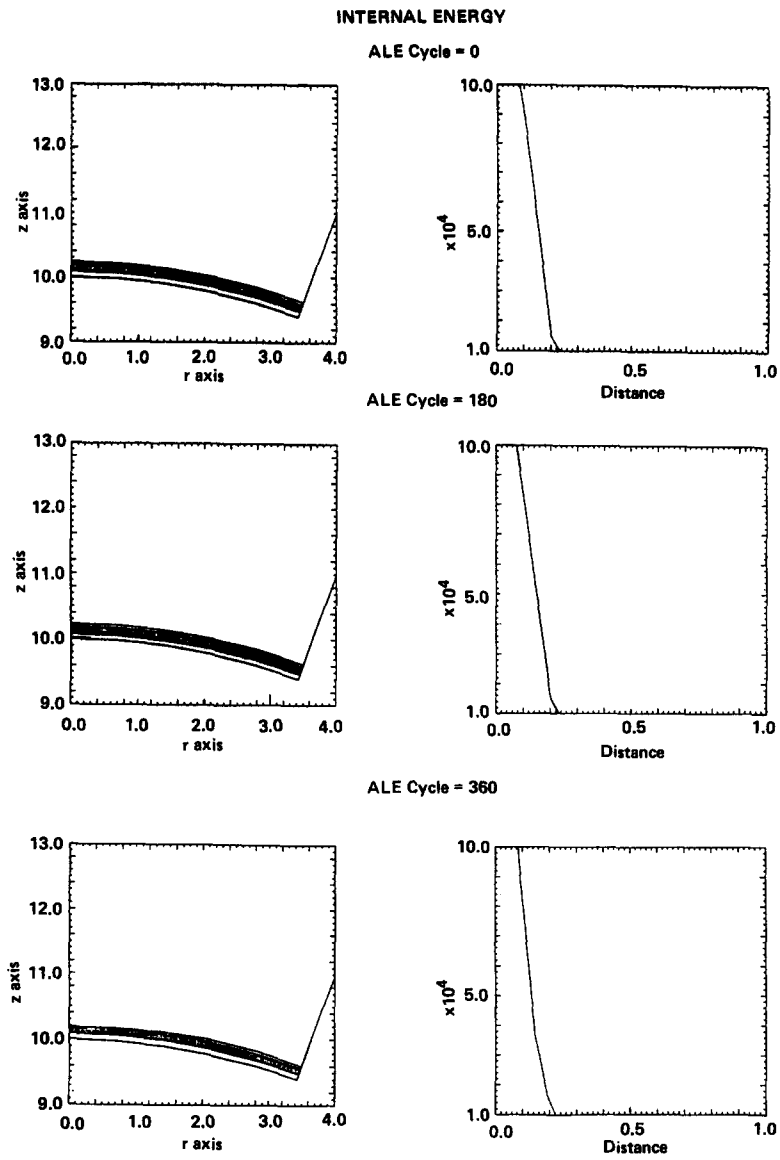

Fig. 11. Contour and profile plots of the internal energy at 0, 180 and 360 major ALE cycles.

where for the ALE problem we choose $\alpha = 1.1$, $\beta = -0.2$, $\gamma = 0.07$, $\delta = 0.1$, $\epsilon = 0.95$ and $\phi = 0.05$. The last step was to introduce a basis function in this transformed system:

$$g_j = (d_j^2 + r_j^2)^{1/2}, \tag{32}$$

where

$$d_j^2 = u_j^2 + v_j^2. \tag{33}$$

Such transformations greatly improved the accuracy, especially at 180 ALE cycles which is an extreme case of "track" data, see Fig. 8.

5. A PROPOSED HYBRID SCHEME

We propose to use a general hybrid scheme for scattered data in which MQ will be the initial interpolant over steep as well as shallow regions. MQ does not represent well relatively flat functions since the expansion requires very flat basis functions requiring very large r^2 parameters

which leads to severe ill-conditioning of the MQ coefficient matrices. Carlson's [30] adaptation of Foley's [20, 24] multistage scheme will be used as a corrector in the shallow gradient regions.

The Foley–Carlson scheme will be described. A scattered data interpolant is used to obtain an initial estimate on a rectangular grid. Using Carlson's bivariate monotonic cubic Hermite splines, local monotonicity errors will be corrected. The function over the rectangular grid is called F_1.

The next stage deals with the original scattered data at the locations, $\mathbf{x}_k$ and the function values, $z(\mathbf{x}_k)$. Then a new set of values, F_2, at $\mathbf{x}_k$ is formed as

$$F_2(\mathbf{x}_k) = F_1(\mathbf{x}_k) - z(\mathbf{x}_k). \tag{34}$$

F_2 will be a new scattered data interpolant which deals with errors between F_1 and z, such as Duchon's [10, 11] or Franke's [7] thin plate splines. This new interpolant is added to F_1. The new interpolant F is given by

$$F(\mathbf{x}_k) = F_1(\mathbf{x}_k) + F_2(\mathbf{x}_k), \tag{35}$$

where F_2 is a small correction function.

F_1 is made monotonic, and the process is repeated until the errors are sufficiently small. Thus one has a hybrid interpolation scheme which is monotonic and accurate for all surfaces, ranging to the very flat to the very steep.

We have found the MQ coefficient matrices can have large condition numbers from two primary sources. The first source is too many similar entries from similar distances and large r^2 parameters. The second source is due to the fact that the condition number of a full matrix increases as N increases. For this reason, we have advocated domain decomposition to not only reduce the condition number, but to greatly reduce the computational effort.

Dyn and Levin [31] and Dyn *et al.* [32] have used both MQ and thin plate splates as a global scheme containing up to 121 points. They developed an iterative scheme based on preconditioning the coefficient matrix. The conditioning matrix is constructed from triangulation of the data points which annihilate all polynomials of degree $<m$ on the data set. They were able to decrease the MQ coefficient matrix of size 121×121 by a factor of 200.

6. SUMMARY

One of the basic assumptions in fluid-dynamics is that the conservative form densities (mass, momentum components and energy) are represented by some unknown piecewise continuous functions. In either physical measurements or numerical simulations, our information about such variables is discrete and finite. From this limited discrete information, we hope to uncover the underlying unknown piecewise continuous behavior so we may predict the vlaues of a variable anywhere in the domain. In addition, we are able to deduce their appropriate partial derivatives, divergences, or integrals.

We have focused upon a very promising method of approximating functions in R^n, called multiquadric (MQ) developed by Hardy [12, 13]. MQ is a general, grid-free, scattered data approximation given by an expansion in terms of upper hyperboloids, each of which is continuously differentiable. The basis functions depend only upon distances between pairs of points.

Madych and Nelson [27] have proved the theoretical justification for MQ's performance. They show for all conditionally positive definite interpolating functions (such as the MQ basis functions), there exists a semi-norm which is minimized by all such interpolating functions for distinct data points, $\mathbf{x}_1, \mathbf{x}_2, \ldots, \mathbf{x}_N$ in R^n.

In this paper, we have extended the original Hardy scheme in three areas. First, we permit the basis function shape parameter, r^2, to vary monotonically. This gives a set of basis functions whose shapes vary from flat sheets to rounded cones in R^n. Second, we use domain decomposition and blending to change a global surface fitting problem into overlapping quasi-local problems. Such decomposition has the additional benefit of rendering the quasi-local MQ coefficient matrix better conditioned with smaller rank. Third, we found that the "track" data problem (data which is closely spaced in one direction and widely spaced in the orthogonal direction) can be treated accurately by transformations which "randomize" the transformed independent variables.

We have demonstrated in several two-dimensional examples over both gridded and scattered data that MQ is an exceptionally accurate interpolation scheme, as compared to exact solutions, expecially in regions where the gradients are rather steep. With such approximate functions, partial derivatives were calculated and found to agree very well with exact solutions. Foley [20] used Mq on three- and four-dimensional data problems also with satisfaction.

MQ has been also used in a dynamic example without significant degradation of its performance. In one example, MQ was used as a spatial interpolant to remap dependent variable to different locations as an underlying mesh underwent distortion in an arbitrary Lagrangian–Eulerian (ALE) remapping scheme. At maximum grid distortion the zone centers were arranged in a typical "track" data configuration or zones having very poor cell aspect ratios. We have found that after 360 major (2160 minor) remappings the contours and profiles were essentially preserved. MQ was also used to solve parabolic, hyperbolic and elliptic partial differential equations. These results are presented in a separate paper.

Accuracy and computational expense are important considerations in choosing one scheme over another. Just because its operation count per node is relatively small, low order finite difference schemes can become prohibitive in two and three dimensions. Such schemes converge very slowly and the truncation errors are reduced only be refining the grid, thereby rapidly increasing the total number of nodes required.

Further research using MQ as a tool for computational fluid-dynamics is advocated for several reasons. MQ is a very high order continuously differentiable spatial discretization scheme which performs well on scattered and gridded data. Fewer points are required in MQ than in low order finite difference or element schemes. Tensor product meshes are not required in higher dimensions, thus simplifying problems with irregular physical boundaries. MQ does not have the connectivity restrictions associated with local finite difference or element schemes. Moving node and Lagrangian schemes based on such local methods with a specific connectivity may give problems with tangled zones or negative areas and volumes. Points may be added or deleted simply using MQ since connectivity is not a problem.

Research is still required to determine the optimal strategy using MQ in applications problems. We do not have the years of collective wisdom to make informed judgments as with finite element schemes.

Acknowledgements—Work performed under the auspices of the U.S. Department of Energy by the Lawrence Livemore National Laboratory under Contract No. W-7405-ENG-48, and partially supported by the Army Research Office, Contract No. MIPR-ARO 124-84.

REFERENCES

1. F. N. Fritsch and R. E. Carlson, Monotone piecewise cubic interpolation. *SIAM Jl numer. Analysis* **17,** 238–246 (1980).
2. R. E. Carlson and F. N. Fritsch, Monotone piecewise bicubic interpolation. *SIAM J numer. Analysis* **22,** 386–400 (1982).
3. J. M. Hyman, Accurate monotonicity preserving cubic interpolation. *SIAM Jl Sci. Stat. Comput.* **4,** 645–654 (1983).
4. R. L. Dougherty, A. S. Edelman and J. M. Hyman, Positivity, monotonicity, or convexity-preserving cubic and quintic Hermite interpolation. *LA-UR-85-2877* (submitted to *SIAM Jl numer. Analysis*).
5. M. Berger and J. Oliger, Adaptive mesh refinement for hyperbolic partial differential equations. *J. Comput. Phys* **53,** 484–512 (1984).
6. B. van Leer, Toward the ultimate conservation scheme, I. *J. Comput. Phys.* **14,** 361–370 (1974); II *J. Comput. Phys.* **23,** 263–275; III *J. Comput. Phys.* **23,** 276–299 (1975).
7. R. Franke, Scattered data interpolation: test of some methods. *Math. Comput.* **38,** 181–200 (1982).
8. J. A. Foley, Smooth multivariate interpolation to scattered data. Ph.D. Dissertation, Arizona State University (1979).
9. T. A. Foley and G. M. Nielson, Multivariate interpolation to scattered data using delta iteration, in *Approximation Theory III* (Ed. E. W. Cheney), pp. 419–424. Academic Press, New York (1980).
10. J. Duchon, Fonctions—spline du type plaque mince en dimension 2. Report #231, Université de Grenoble (1975).
11. J. Duchon, Fonctions—spline a energie invariante par rotation. Report #27, Université de Grenoble (1976).
12. R. L. Hardy, Multiquadric equations of topography and other irregular surfaces. *J. geophys. Res.* **176,** 1905–1915 (1971).
13. R. L. Hardy, Research results in the application of multiquadric equations to surveying and mapping problems. *Survg Mapp.* **35,** 321–332 (1975).
14. A. E. Tarwater, A parameter study of Hardy's multiquadric method for scattered data interpolation. UCRL-54670, Sept. (1985).
15. C. A. Micchelli, Interpolation of scattering data: distance matrices and conditionally positive definite functions. *Constr. Approx.* **2,** 11–22 (1986).
16. G. A. Korn and T. M. Korn, *Mathematical Handbook for Scientists and Engineers.* McGraw-Hill, New York (1968).

17. P. Lancaster and K. Salkauskas, *Curve and Surface Fitting: An Introduction*. Academic Press, New York (1986).
18. S. Stead, Estimation of gradients from scattered data. *Rocky Mount. J. Math.* **14,** 265–279 (1984).
19. E. J. Kansa, Application of Hardy's multiquadric interpolation to hydrodynamics. *Proc. 1986 Multiconf. Computer Simulation*, Vol. 4, pp. 111–117, Jan. (1986).
20. T. A. Foley, Interpolation and approximation of 3-D and 4-D scattered data. *Computers Math. Applic.* **13,** 711–740 (1987).
21. R. Franke, Recent advances in the approximation of surfaces from scattered data. NPS-53-87-001 Naval Post Graduate School, Monterey, Calif., Dec. (1986).
22. R. Schiro and G. Williams, An adaptive application of multiquadric interpolants for numerically modeling large numbers of irregularly spaced hydrographic data. *Survg Mapp.* **44,** 365–381 (1984).
23. A. Damon, Extensions of smoothing spline methods using generalized cross validation. Cranfield Institute of Technology, Technical Note COMA 3/86 (1986).
24. T. A. Foley, Scattered data interpolation and approximation with error bounds, Vol. 3. *Comput. Aided. Geometric Des.* **3,** 163–177 (1986).
25. R. L. Hardy and S. A. Nelson, A multiquadric–biharmonic representation and approximation of disturbing potentials. *Geophys. Res. Lett.* **13,** 18–21 (1986).
26. R. L. Hardy, *Surface Fitting with Biharmonic and Harmonic Models*, pp. 135–147. NASA Workshop on Surface Fitting, Texas A&M University Press, May (1982).
27. W. R. Madych and S. A. Nelson, Multivariate interpolation: a variational theory. *J. Approx. Theory Applic.* (in press).
28. F. G. Blake, Spherical wave propagation in solid media. *J. acoust. Soc. Am.* **24,** 211–215 (1952).
29. J. K. Dukowicz and J. W. Kodis Accurate conservative remapping (REZONING) for arbitrary Lagrangian–Eulerian computations. *SIAM Jl Sci. Stat. Comput.* **8,** 305–320 (1987).
30. R. E. Carlson, Private communication, LLNL (1986).
31. N. Dyn and D. Levin, Iterative solution of systems originating from integral equations and surface interpolation. *SIAM Jl numer. Analysis* **20,** 377–390 (1983).
32. N. Dyn, D. Levin and S. Rippa, Numerical procedures for surface fitting of scattered data by radial functions. *SIAM Jl Sci. Stat. Comput.* **7,** 639–659 (1986).